Proc. Natl. Acad. Sci., India, Sect. A Phys. Sci. (July–September 2015) 85(3):421–426
DOI 10.1007/s40010-015-0217-1

RESEARCH ARTICLE

Study of Flow and Heat Transfer on a Stretching Surface in a Rotating Casson Fluid

Adnan Saeed Butt[1] · **Asif Ali** [1,2] · **Ahmer Mehmood**[3]

Received: 13 July 2014 / Revised: 8 February 2015 / Accepted: 23 February 2015 / Published online: 14 July 2015

Abstract The steady, boundary layer flow and heat transfer on a stretching surface in rotating fluid has been examined. Using suitable similarity transformations, the partial differential equations governing the flow and heat transfer phenomenon convert to a system of non-linear ordinary differential equations. The obtained equations are solved by using the shooting technique with fifth order Runge–Kutta–Fehlberg method. The parameters involving in the problem are Casson fluid parameter β, non-dimensional parameter λ that signifies the importance of rotation rate to stretching rate and Prandtl number Pr. The effects of these parameters on physical quantities such as velocity and temperature profiles, skin frictions and Nusselt number are inspected with the aid of graphs and tables.

Keywords Rotating casson fluid · Stretching surface · Heat transfer

1 Introduction

The boundary layer flow induced by the continous stretching of a surface about a fixed point was initially investigated by Crane [1]. He assumed that the surface is stretching with a velocity proportional to the linear distance from the fixed point. We need heat transfer phenomena in flow over a stretching sheet [2–15].

The rotating fluid flows have applications in industrial processes, astrophysical and geophysical phenomenon, biomechanics, cosmic fluid dynamics, in the design of turbines and turbomechanics and rotating heat exchangers. The migration of underground water and movement of petrol, oil and gas through the reservoirs are some examples of rotating flows. Deka et al. [16] examined the viscous, incompressible rotating fluid flow induced by uniformly accelerated flat surface. Wang [17] investigated the flow over a stretching surface in a rotating viscous fluid and obtained the self-similar solutions. The magnetic field effects on flow and heat transfer characteristics on a stretching sheet in a rotating fluid were examined by Takhar et. al. [18]. The unsteady flow of a viscous fluid over a surface stretching linearly in its plane in a rotating fluid was analyzed by Rajeswari and Nath [19] and Nazar et al. [20]. Abbas et al. [21] extended the Nazar's problem [20] by considering the effects of magnetic field and obtained the solution of the problem by using the implicit finite difference scheme known as Keller box method. Zaimi et al. [22] studied the fluid flow due to stretching of a surface in rotating viscoelastic fluid and found that viscoelastic parameter has increasing effect on velocity in x-direction whereas opposite behavior is observed for velocity in y-direction.

The fluids found in nature and industry exhibit non-Newtonian behavior and it is not possible to represent the behavior of these fluids by classical Navier–Stoke's equations. Different models have been proposed by the rheologists as no single constitutive equation could be found to describe all the properties of non-Newtonian fluids. Of these models, Casson fluid model represents a shear

✉ Adnan Saeed Butt
adnansaeedbutt85@gmail.com

1 Department of Mathematics, Quaid-i-Azam University, Islamabad 44000, Pakistan

2 Department of Mathematics and Natural Sciences, Prince Mohammad Bin Fahd University, Al Khobar 31952, Saudi Arabia

3 Department of Mathematics, International Islamic University, Islamabad 44000, Pakistan

thinning fluid which is assumed to have infinite viscosity at zero rate of shear [23]. The flow and heat transfer characteristics of Casson fluid from different physical and mathematical aspects have been investigated by several researchers [24–32].

The present study focusses on boundary layer flow and heat transfer due to a surface stretching in a rotating Casson fluid. A complete parametric study is presented through graphs and tables.

2 Mathematical Formulation

Consider a steady, incompressible boundary layer flow caused by the stretching of a heated surface in a rotating Casson fluid. The flow is three dimensional due to the presence of Coriolis force. It is assumed that the surface is stretching in the x direction with a velocity proportional to the distance from the origin. Let (u, v, w) denote the velocity components in the (x, y, z) directions with the axes rotating at an angular velocity Ω in the z direction (see Fig. 1). The temperature of the stretching surface is kept constant at T_w and the far away fluid is assumed to have the temperature T_∞. The rheological model that characterizes Casson fluid is given by :

$$\tau_{ij} = \begin{cases} 2\left(\mu_B + \dfrac{p_y}{\sqrt{2\pi}}\right)e_{ij}, & \pi > \pi_c \\ 2\left(\mu_B + \dfrac{p_y}{\sqrt{2\pi_c}}\right)e_{ij}, & \pi < \pi_c \end{cases}, \tag{2.1}$$

where τ_{ij} is the Cauchy stress tensor, $\pi = e_{ij}e_{ij}$ is the product of components of deformation rate with itself, e_{ij} is the (i, j)th component of deformation rate, π_c is the critical value of this product based on the non-Newtonian model, μ_B is the plastic dynamic viscosity of the non-Newtonian model and p_y is the yield stress of fluid and then the governing equations for the continuity, momentum and energy are:

$$\frac{\partial u}{\partial x} + \frac{\partial v}{\partial y} + \frac{\partial w}{\partial z} = 0, \tag{2.2}$$

$$u\frac{\partial u}{\partial x} + v\frac{\partial u}{\partial y} + w\frac{\partial u}{\partial z} - 2\Omega v = -\frac{1}{\rho}\frac{\partial p}{\partial x} + \nu\left(1 + \frac{1}{\beta}\right)\nabla^2 u, \tag{2.3}$$

$$u\frac{\partial v}{\partial x} + v\frac{\partial v}{\partial y} + w\frac{\partial v}{\partial z} + 2\Omega u = -\frac{1}{\rho}\frac{\partial p}{\partial y} + \nu\left(1 + \frac{1}{\beta}\right)\nabla^2 v, \tag{2.4}$$

$$u\frac{\partial w}{\partial x} + v\frac{\partial w}{\partial y} + w\frac{\partial w}{\partial z} = -\frac{1}{\rho}\frac{\partial p}{\partial z} + \nu\left(1 + \frac{1}{\beta}\right)\nabla^2 w, \tag{2.5}$$

$$u\frac{\partial T}{\partial x} + v\frac{\partial T}{\partial y} + w\frac{\partial T}{\partial z} = \frac{k}{\rho c_p}\nabla^2 T. \tag{2.6}$$

The boundary conditions related to the present problem are

$$\left.\begin{array}{l} u = u_w(x) = ax, v = 0,\ w = 0,\ T = T_w \quad \text{at} \quad z = 0, \\ u \to 0, v \to 0,\ T \to T_\infty \quad \text{at}\ z \to \infty. \end{array}\right\} \tag{2.7}$$

Here $a > 0$ is a constant, $\beta = \frac{\mu_B\sqrt{2\pi_c}}{p_y}$ is the Casson fluid parameter, ν is the kinematic viscosity, k is the thermal conductivity, c_p is the specific heat of the fluid at a constant pressure, ρ is the density and T is the temperature of the fluid. Introducing the following similarity variables:

$$\begin{array}{l} u = axf'(\eta),\ v = axg(\eta),\ w = -\sqrt{a\nu}f(\eta), \\ \eta = \sqrt{\dfrac{a}{\nu}}z,\ \theta = \dfrac{T - T_\infty}{T_w - T_\infty}. \end{array} \tag{2.8}$$

By substituting (2.8) in Eqs. (2.2–2.5), Eq. (2.2) is identically satisfied and Eqs. (2.3, 2.4, 2.6) become

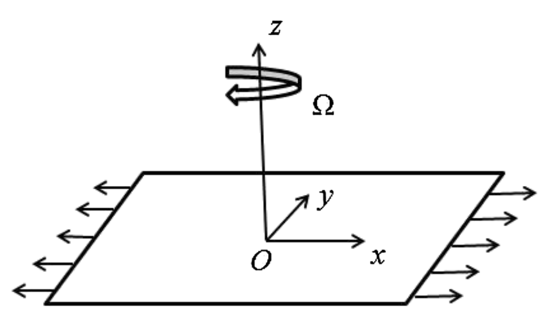

Fig. 1 Schematic diagram of the problem

Table 1 Comparison of obtained values of $f''(0)$ with those of Wang [17] and Nazar et al. [20] when $\beta \to \infty$

λ	$f''(0)$ [17]	$f''(0)$ [20]	$f''(0)$ *Present*	*Error* $= \left\lvert f''(0)_{[17]} - f''(0)_{Present} \right\rvert$
0.0	−1.0000	−1.0000	−1.0000	0
0.5	−1.1384	−1.1384	−1.1384	0
1.0	−1.3250	−1.3250	−1.3250	0
2.0	−1.6523	−1.6523	−1.6523	0

Table 2 Comparison of obtained values of $g'(0)$ with those of Wang [17] and Nazar et al. [20] when $\beta \to \infty$

λ	$g'(0)$ [17]	$g'(0)$ [20]	$g'(0)$ *Present*	$Error = \left\vert g'(0)_{[17]} - g'(0)_{Present} \right\vert$
0.0	0.0000	0.0000	0.0000	0
0.5	−0.5128	−0.5128	−0.5128	0
1.0	−0.8371	−0.8371	−0.8371	0
2.0	−1.2873	−1.2873	−1.2873	0

Table 3 Comparison of obtained values of $\theta'(0)$ with those of Wang [17] when $\beta \to \infty$ with error defined as $Error = \vert \theta'(0)[17] - \theta'(0)_{Present} \vert$

λ	$Pr = 0.7$			$Pr = 2.0$			$Pr = 7.0$		
	$\theta'(0)$ [17]	$\theta'(0)$ *Present*	*Error*	$\theta'(0)$ [17]	$\theta'(0)$ *Present*	*Error*	$\theta'(0)$ [17]	$\theta'(0)$ *Present*	*Error*
0.0	−0.455	−0.454	1E−3	−0.911	−0.911	0	−1.894	−1.895	1E−3
0.5	−0.390	−0.389	1E−3	−0.853	−0.852	1E−3	−1.850	−1.851	1E−3
1.0	−0.321	−0.321	0	−0.770	−0.770	0	−1.788	−1.788	0
2.0	−0.242	−0.242	0	−0.638	−0.638	0	−1.664	−1.664	0

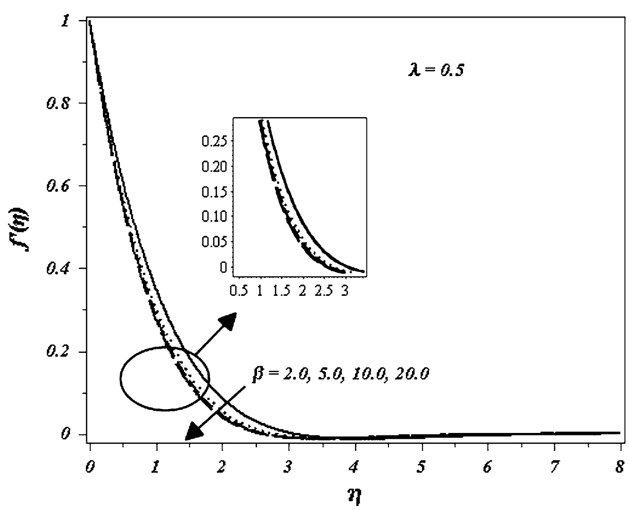

Fig. 2 Influence of Casson fluid parameter β on $f'(\eta)$ when $\lambda = 0.5$

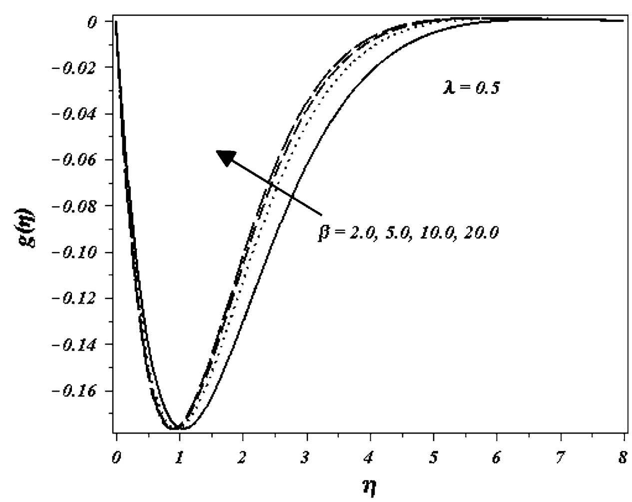

Fig. 3 Influence of Casson fluid parameter β on $g(\eta)$ when $\lambda = 0.5$

$$\left(1+\frac{1}{\beta}\right)f''' + ff'' - f'^2 + 2\lambda g = 0, \tag{2.9}$$

$$\left(1+\frac{1}{\beta}\right)g'' + fg' - f'g - 2\lambda f' = 0, \tag{2.10}$$

$$\theta'' + Prf\theta' = 0, \tag{2.11}$$

where $\lambda = \Omega/a$ is the ratio of rate of rotation to stretching rate and $Pr = \mu c_p/k$ is the Prandtl number. The boundary conditions (2.7) in dimensionless form are

$$\left.\begin{array}{l} f'(0) = 1, f(0) = 0, g(0) = 0, \theta(0) = 1, \\ f'(\infty) = 0, g(\infty) = 0, \theta(\infty) = 0. \end{array}\right\} \tag{2.12}$$

The skin friction coefficients along x and y directions, i.e., C_{fx} and C_{fy} are:

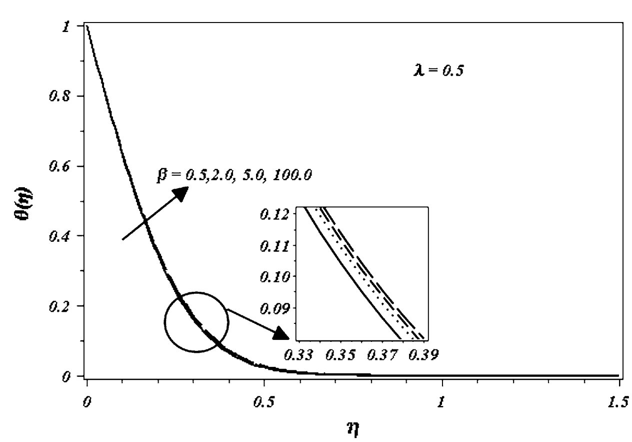

Fig. 4 Influence of Casson fluid parameter β on $\theta(\eta)$ when $\lambda = 0.5$

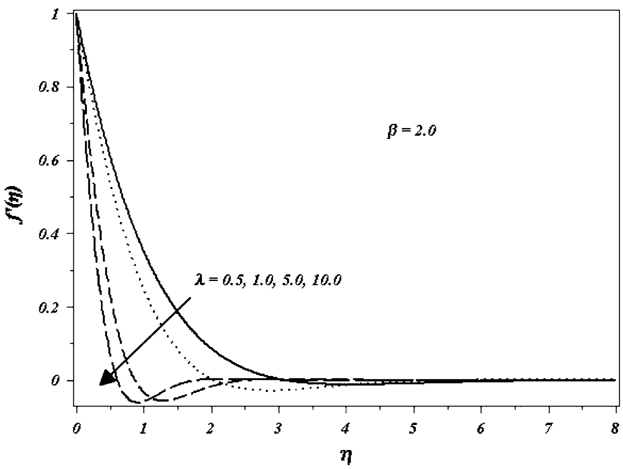

Fig. 5 Influence of rotation parameter λ on $f'(\eta)$ when $\beta = 2.0$

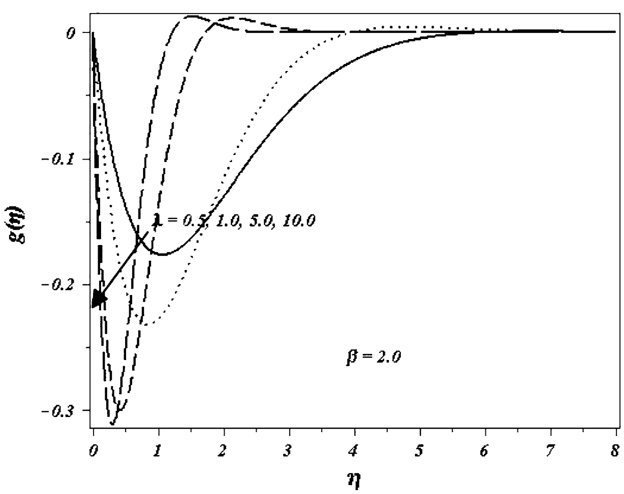

Fig. 6 Influence of rotation parameter λ on $g(\eta)$ when $\beta = 2.0$

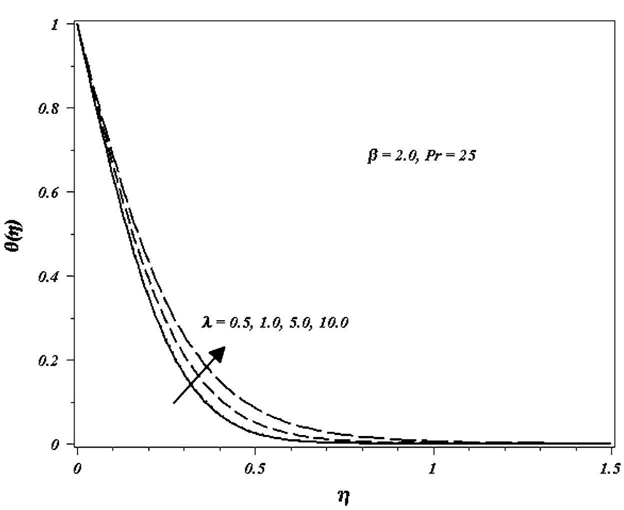

Fig. 7 Influence of rotation parameter λ on $\theta(\eta)$ when $\beta = 2.0$

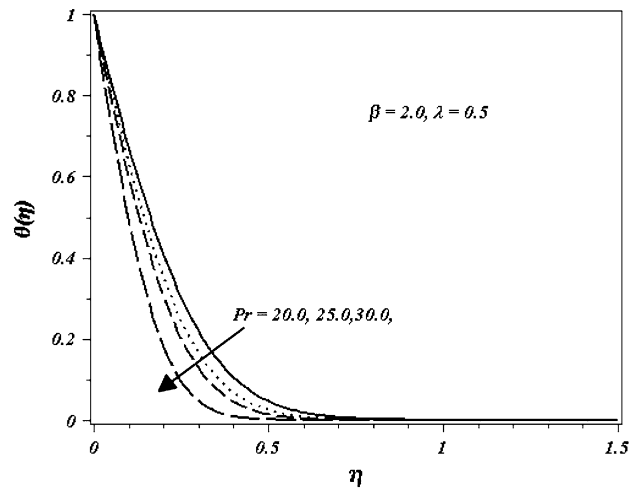

Fig. 8 Influence of Prandtl number Pr on $\theta(\eta)$ when $\beta = 2.0$, $\lambda = 0.5$

$$C_{fx} = \frac{\tau_{wx}}{\rho u_w^2}, \quad C_{fy} = \frac{\tau_{wy}}{\rho u_w^2}, \tag{2.13}$$

where τ_{wx} is the surface shear stress along the x direction and τ_{wy} is the surface shear stress along the y direction and are defined as

$$\begin{aligned} \tau_{wx} &= \left(\mu_B + \frac{p_y}{\sqrt{2\pi}}\right)\left(\frac{\partial u}{\partial z}\right)_{z=0}, \\ \tau_{wy} &= \left(\mu_B + \frac{p_y}{\sqrt{2\pi}}\right)\left(\frac{\partial v}{\partial z}\right)_{z=0}. \end{aligned} \tag{2.14}$$

Using Eqs. (2.14) and (2.8), we obtain

$$Re_x^{1/2} C_{fx} = \left(1 + \frac{1}{\beta}\right) f''(0), \quad Re_x^{1/2} C_{fy} = \left(1 + \frac{1}{\beta}\right) g'(0). \tag{2.15}$$

The local Nusselt number Nu_x is defined as

$$Nu_x = \frac{x q_w}{k(T_w - T_\infty)}, \tag{2.16}$$

where the heat flux q_w is given as

$$q_w = -k \frac{\partial T}{\partial z}\bigg|_{z=0}. \tag{2.17}$$

Substituting the value of q_w into Eq. (2.16), we have the non-dimensional of Nusselt number as

$$Re_x^{-1/2} Nu_x = -\theta'(0). \tag{2.18}$$

3 Numerical Results and Discussion

A numerical study of flow and heat transfer on a stretching sheet in a rotating Casson fluid has been carried out and the non-linear differential equations (2.9–2.11) with the boundary conditions (2.12) are solved with the help of

Table 4 Numerical values of $Re_x^{1/2}C_{fx}$ and $Re_x^{1/2}C_{fy}$ for different values of rotation parameter λ and Casson fluid parameter β

λ	β	$Re_x^{1/2}C_{fx}$	$Re_x^{1/2}C_{fy}$
0.5	2.0	−1.394220	−0.628002
1.0		−1.622822	−1.025232
5.0		−2.927312	−2.633846
10.0		−4.007462	−3.797251
0.5	2.0	−1.394220	−0.628002
	5.0	−1.247034	−0.561702
	10.0	−1.193944	−0.537788
	20.0	−1.166493	−0.525423

Table 5 Numerical values of $Re_x^{-1/2}Nu_x$ for different values of rotation parameter λ, Casson fluid parameter β and Prandtl number Pr

λ	β	Pr	$Re_x^{-1/2}Nu_x$
0.5	2.0	25.0	3.786167
1.0			3.746427
5.0			3.492736
10.0			3.241317
0.5	2.0	1.0	3.786167
	5.0		3.761330
	10.0		3.750813
	20.0		3.744985
0.5	2.0	20.0	3.322708
		25.0	3.786167
		30.0	4.167490
		50.0	5.440473

shooting method with fifth order Runge–Kutta–Fehlberg method. The scheme has been carried out in symbolic software *MAPLE*. The boundary conditions defined at infinity are replaced by a sufficiently large value $\eta = \eta_{\max}$. In the present study $\eta_{\max}$ is taken to be 15 for all values of involved physical parameters. The accuracy up to 6 decimal places is chosen to be the convergence criteria and step size is taken as $\Delta\eta = 0.001$. In order to check the accuracy and validity of the obtained results, Tables 1, 2 and 3 list the obtained values of $f''(0)$, $g'(0)$ and $\theta'(0)$ and compared with those of Wang [17] and Nazar [20] under limiting conditions.

The effects of the Casson fluid parameter β on the similarity velocity profiles $f'(\eta)$ and $g(\eta)$ in x and y directions are presented in Figs. 2 and 3. It is noticed that the velocity profiles $f'(\eta)$ and $g(\eta)$ decrease with an increase in the value of Casson fluid parameter β. This is due to the fact that the introduction of tensile stress due to elasticity creates resistance in the fluid flow which results in reduction of velocities. For higher values of β, the momentum boundary layer thickness decreases. On the otherhand, an increase in thermal boundary layer thickness is observed with increase in β as shown in Fig. 4.

Figure 5 exhibits the impact of rotation parameter λ on similarity velocity profile $f'(\eta)$ in x-direction. An increase in the value of λ results in decrease in the velocity $f'(\eta)$. For small values of λ, i.e for $0 \le \lambda \le 1$, the stretching rate of surface is more than or equal to the fluid rotation rate and a monotonically exponential decay in $f'(\eta)$ is observed. On the otherhand, for large values of λ, i.e for $\lambda > 1$, the fluid rotation rate is significant and an oscillatory decay in velocity $f'(\eta)$ is noticed. The effects of variation in rotation parameter λ on similarity velocity profile $g(\eta)$ in y-direction is shown in Fig. 6. The velocity profile $g(\eta)$ is increased oscillatory for large values of λ whereas there is no oscillation in velocity for smaller values. Figure 7 exhibits the effects of rotation parameter λ on the temperature profiles $\theta(\eta)$. An increase in thermal boundary layer thickness is noticed with increase in λ. Thus, increase in rotation parameter results in rise in the fluid temperature. Figure 8 indicates that increasing the Prandtl number Pr results in decrease in the thermal boundary layer thickness.

The effects of variation in rotation parameter λ and Casson fluid parameter β on the skin friction coefficients in the x- and y-directions, $Re_x^{1/2}C_{fx}$ and $Re_x^{1/2}C_{fy}$ are presented in Table 4. It can be seen that there is an increase in $Re_x^{1/2}C_{fx}$ and $Re_x^{1/2}C_{fy}$ as the value of Casson fluid parameter β increases. Moreover, as the value of rotation parameter λ increases, the values of the skin friction coefficients in x and y directions decrease thus resulting in reduction in the thickness of momentum boundary layer. Table 5 illustrates the effects of rotation parameter λ, Casson fluid parameter β and Prandtl number Pr on local Nusselt number $Re_x^{-1/2}Nu_x$. A drop in heat transfer rate is observed as the values of the rotation parameter λ and Casson fluid parameter β increase whereas there is an enhancement in the heat transfer coefficient with increase in the value of Prandtl number.

4 Conclusions

We investigate the flow and heat transfer phenomenon on a sheet stretching in a rotating Casson fluid. The exact similarity solutions are obtained and the results are analyzed and interpreted. The main observations of the study are:

(a) The similarity velocity profiles $f'(\eta)$ and $g(\eta)$ in x and y directions decrease as the value of Casson fluid parameter β increases.
(b) The velocity profile $f'(\eta)$ in x direction decrease with increase in rotation parameter λ.
(c) An increase in the thermal boundary layer thickness is observed with increase in Casson fluid parameter β

and rotation parameter λ whereas reduction in thermal boundary layer thickness is notices as the value of Prandtl number Pr increases.

(d) The skin friction coefficients $Re_x^{1/2}C_{fx}$ and $Re_x^{1/2}C_{fy}$ in x and y directions decrease with rotation parameter λ. On the otherhand, an increasing effect on $Re_x^{1/2}C_{fx}$ and $Re_x^{1/2}C_{fy}$ is observed as the Casson fluid parameter β increases.

(e) The local Nusselt number $Re_x^{-1/2}Nu_x$ decreases with increase in Casson fluid parameter β and rotation parameter λ whereas Prandtl number Pr has increasing effect on heat transfer coefficient.

References

1. Crane LJ (1977) Flow past a stretching slate. Z Angew Math Phys 21:645–647
2. Gupta PS, Gupta AS (1977) Heat and mass transfer on a stretching sheet with suction or blowing. Can J Chem Eng 55:744–746
3. Grubka J, Bobba KM (1985) Heat transfer characteristics of a continuous stretching surface with variable temperature. Trans ASME J Heat Transf 107:248–250
4. Banks WHH (1983) Similarity solutions of the boundary layer equation for a stretching wall. J Mech Theor Appl 2:375–392
5. Ali ME (1995) On thermal boundary layer on a power law stretched surface with suction or injection. Int J Heat Mass Flow 16:280–290
6. Elbashbeshy EMA (1998) Heat transfer over a stretching surface with variable heat flux. J Phys D Appl Phys 31:1951–1955
7. Sriramalu A, Kishan N, Anand RJ (2001) Steady flow and heat transfer of a viscous incompressible fluid flow through porous medium over a stretching sheet. J Energy Heat Mass Transf 23:483–495
8. Andersson HI (2002) Slip flow past a stretching surface. Acta Mech 158:121–125
9. Wang CY (2002) Flow due to a stretching boundary with partial slip-an exact solution of the Navier-Stokes equations. Chem Eng Sci 57:3745–3747
10. Mehmood A, Ali A, Shah T (2008) Unsteady boundary-layer viscous flow due to an impulsively started porous plate. Can J Phys 86:1079–1082
11. Mehmood A, Ali A (2008) Analytic solution of three-dimensional viscous flow and heat transfer over a stretching flat surface by homotopy analysis method. ASME J Heat Transf 130:121701–121707
12. Ali A, Mehmood A (2008) Homotopy analysis of unsteady boundary layer flow adjacent to permeable stretching surface in a porous medium. Commun Nonlinear Sci Numer Simul 13: 340–349
13. Fang T, Zhang J, Yao S (2009) Slip MHD flow over a stretching sheet-an exact solution. Commun Nonlinear Sci Numer Simul 14:3731–3737
14. Mehmood A, Ali A (2010) Injection flow past a porous plate: solution to an unsolved problem. Int J Nonlinear Sci Numer Simul 11:511–518
15. Yao S, Fang T, Zhong Y (2011) Heat transfer of a generalized stretching/ shrinking wall problem with convective boundary conditions. Commun Nonlinear Sci Numer Simul 16:752–760
16. Deka RK, Gupta AS, Takhar HS, Soundalgekar VM (1999) Flow past an accelerated horizontal plate in a rotating fluid. Acta Mech 138:13–19
17. Wang CY (1988) Stretching a surface in a rotating fluid. Z Angew Math Phys 39:177–185
18. Takhar HS, Chamkha AJ, Nath G (2003) Flow and heat transfer on a stretching surface in a rotating fluid with a magnetic field. Int J Therm Sci 42:23–31
19. Rajeswari V, Nath G (2004) Unsteady flow over a stretching surface in a rotating fluid. Int J Eng Sci 30:121–128
20. Nazar R, Amin N, Pop I (2004) Unsteady boundary layer flow due to a stretching surface in a rotating fluid. Mech Res Commun 31:121–128
21. Abbas Z, Javed T, Sajid M, Ali N (2010) Unsteady MHD flow and heat transfer on a stretching sheet in a rotating fluid. J Taiwan Inst Chem Eng 41:644–650
22. Zaimi K, Ishak A, Pop I (2013) Stretching surface in rotating viscoelastic fluid. Appl Math Mech Engl Ed 34:945–952
23. Casson NA (1959) A flow equation for pigment oil suspension of printing ink type. In: Mill CC (ed) Rheology of dispersed system. Pergamon Press, Oxford
24. Eldabe NTM, Salwa MGE (1995) Heat transfer of MHD non-newtonian casson fluid flow between two rotating cylinders. J Phys Soc Jpn 64:41–64
25. Boyd J, Buick JM, Green S (2007) Analysis of the Casson and Carreau-Yasuda Non-Newtonian blood models in steady and oscillatory flow using the Lattice Boltzmann Method. Phys Fluids 19:93–103
26. Bhargava R, Takhar HS, Rawat S, Bèg TA, Bèg OA (2007) Finite element solutions for Non-Newtonian Pulsatile flow in a Non-Darician porous medium conduit. Nonlinear Anal Model Control 12:317–327
27. Attia HA, Ahmed MES (2010) Transient MHD couette flow of a Casson fluid between parallel plates with heat transfer. Ital J Pure Appl Math 27:19–38
28. Mukhopadhyay S (2013) Casson fluid flow and heat transfer over a nonlinearly stretching surface. Chin Phys B 27:074701–074705
29. Nandy SK (2013) Analytical solution of MHD stagnation-point flow and heat transfer of Casson fluid over a stretching sheet with partial slip. ISRN Thermodyn 2013:9. doi:10.1155/2013/108264 Article ID 108264
30. Mukhopadhyay S, Mondal IC, Chamkha AJ (2013) Casson fluid flow and heat transfer past a symmetric wedge. Heat Transf Asian Res 42:665–675
31. Tufail MN, Butt AS, Ali A (2014) Heat source/sink effects on Non-Newtonian MHD fluid flow and heat transfer over a permeable stretching surface: Lie group analysis. Indian J Phys 1:75–82
32. Qasim M, Noreen S (2014) Heat transfer in the boundary layer flow of a Casson fluid over a permeable shrinking sheet with viscous dissipation. Eur Phys J Plus 7:129–137